Pace, U., Hanski, E., Salomon, Y., & Lancet, D. (1985) *Nature 316*, 255–258.
Pelosi, P., Baldaccini, N. E., & Pisanelli, A. M. (1982) *Biochem. J. 201*, 245–248.
Pevsner, J., Trifiletti, R. R., Strittmatter, S. M., & Snyder, S. H. (1985) *Proc. Natl. Acad. Sci. U.S.A. 82*, 3050–3054.
Pevsner, J., Reed, R. R., Feinstein, P. G., & Snyder, S. H. (1988) *Science 241*, 336–339.
Pfeuffer, E., Mollner, S., Lancet, D., & Pfeuffer, T. (1989) *J. Biol. Chem. 264*, 18803–18807.
Phillips, T. E., & Boyne, A. F. (1984) *J. Electron Microsc. Tech. 1*, 9–29.
Reese, T. S. (1965) *J. Cell Biol. 25*, 209–230.
Restrepo, D., Miyamoto, T., Bryant, B. P., & Teeter, J. H. (1990) *Science 249*, 1166–1168.
Shirley, S. G., Robinson, C. J., Dickinson, K., Aujla, R., & Dodd, G. H. (1986) *Biochem. J. 240*, 605–607.
Sicard, G., & Holley, A. (1984) *Brain Res. 292*, 283–296.
Sitte, H., Neumann, K., & Edelmann, L. (1986) in *The Science of Biological Specimen Preparation for Microscopy and Microanalysis 1985* (Mueller, M., Becker, R. P., Boyde, A., & Wolose-wick, J. J., Eds.) pp. 103–108, Scanning Electron Microscopy, Inc., AMF O'Hare, Chicago, IL.
Sklar, B. P., Anholt, R. R. H., & Snyder, S. H. (1986) *J. Biol. Chem. 261*, 15538–15543.

Conformational Mobility of His-64 in the Thr-200 → Ser Mutant of Human Carbonic Anhydrase II[†,‡]

Joseph F. Krebs and Carol A. Fierke*
Department of Biochemistry, Duke University Medical Center, Box 3711, Durham, North Carolina 27710
Richard S. Alexander and David W. Christianson*
Department of Chemistry, University of Pennsylvania, Philadelphia, Pennsylvania 19104-6323
Received March 27, 1991; Revised Manuscript Received June 20, 1991

ABSTRACT: The three-dimensional structure of the Thr-200 → Ser (T200S) mutant of human carbonic anhydrase II (CAII) has been determined by X-ray crystallographic methods at 2.1-Å resolution. This particular mutant of CAII exhibits CO_2 hydrase activity that is comparable to that of the wild-type enzyme with a 2-fold stabilization of the $E{\cdot}HCO_3^-$ complex and esterase activity that is 4-fold greater than that of the wild-type enzyme. The structure of the mutant enzyme reveals no significant local changes accompanying the conservative T200S substitution, but an important nonlocal structural change is evident: the side chain of catalytic residue His-64 rotates away from the active site by 105° about χ_1 and apparently displaces a water molecule. The displaced water molecule is present in the wild-type enzyme; however, the electron density into which this water is built is interpretable as an alternate conformation of His-64 with 10–20% occupancy. The rate constants for proton transfer from the zinc–water ligand to His-64 and from His-64 to bulk solvent are maintained in the T200S variant; therefore, if His-64 is conformationally mobile about χ_1 and/or χ_2 during catalysis, compensatory changes in solvent configuration must sustain efficient proton transfer.

Human carbonic anhydrase II (CAII;[1] EC 4.2.1.1) is a zinc metalloenzyme containing one essential metal ion bound to a single polypeptide chain of 260 amino acids [for recent reviews, see Coleman (1986); Lindskog (1986); Silverman and Lindskog (1988), and Christianson (1991)]. The biological function of CAII in the erythrocyte is the hydration of carbon dioxide to form bicarbonate ion plus a proton. Since $k_{cat}/K_M = 1.5 \times 10^8$ M^{-1} s^{-1} for this enzyme, it appears to be one of only a few enzymes for which catalysis approaches the limit of diffusion control. However, since the biological mechanism of CAII requires a proton transfer from the enzyme to bulk solvent, the observed turnover rate of 10^6 s^{-1} requires the participation of buffer—ordinarily, proton transfer from an enzyme-bound group with $pK_a = 7$ to bulk solvent may proceed no faster than 10^3 s^{-1} (Eigen & Hammes, 1963).

The structure of native CAII from human blood has been determined by X-ray crystallographic methods (Liljas et al., 1972) and refined at 2.0-Å resolution (Eriksson et al., 1986, 1988a). The enzyme is roughly spherical and the active site lies at the bottom of a conical cleft about 15 Å deep. Important polar residues in the active site include Thr-199, Thr-200, Glu-106, and His-64; His-94, His-96, His-119, and hydroxide ion coordinate to Zn^{2+}. Additionally, a hydrophobic pocket is adjacent to the zinc–hydroxide species. Of the polar active-site residues, Glu-106 and Thr-199 engage zinc-bound hydroxide in a hydrogen-bond network (Eriksson et al., 1988a; Merz, 1990, 1991), Thr-200 interacts with CO_2 in a proposed

[†] D.W.C. thanks the NIH for Grant GM45614, the NSF for Grant DIR-8821184, the Chicago Community Trust for a Searle Scholar Award, and the Office of Naval Research for a Young Investigator Award. C.A.F. thanks the NIH for Grant GM40602, the American Cancer Society for Grant JFRA-246, and The David and Lucile Packard Foundation for a Fellowship in Science and Engineering.

[‡] The coordinates of T200S CAII, as well as those of the wild-type enzyme, have been deposited in the Brookhaven Protein Data Bank under reference codes 5CA2 and 4CA2, respectively.

[1] Abbrevations: IPTG, isopropyl β-D-thiogalactopyranoside; T200S, Thr-200 → Ser; T200H, Thr-200 → His; CAII, human carbonic anhydrase II; WT, wild type; PNPA, *p*-nitrophenyl acetate; MES, 2-(*N*-morpholino)ethanesulfonic acid; TAPS, [tris(hydroxymethyl)methyl]-3-aminopropanesulfonic acid; HEPES, *N*-(2-hydroxyethyl)piperazine-*N*'-2-ethanesulfonic acid; EDTA, (ethylenedinitrilo)tetraacetic acid; DNSA, dansylamide; ACET, acetazolamide.

0006-2960/91/0430-9153$02.50/0

binding site (Merz, 1990; Liang & Lipscomb, 1990), and His-64 serves as a proton shuttle in the conversion of zinc-bound water into zinc-bound hydroxide (Steiner et al., 1975; Tu et al., 1989; Liang & Lipscomb, 1988). Residue His-64 is about 8 Å from zinc-bound hydroxide and 5 Å away from Thr-200 in the native enzyme; however, His-64 probably interacts with these residues through solvent.

Residue-200 is either threonine, asparagine, or histidine in the known isozymes of carbonic anhydrase; Thr-200 is found in all isozymes II and III (except sheep CAII), whereas His-200 is found in many type I isozymes (Hewett-Emmett & Tashian, 1991). Carbonic anhydrase isozymes exhibit different catalytic efficiencies due to primary sequence variations and the resulting changes in the structure of the active site. Catalytic differences between human carbonic anhydrase II and human carbonic anhydrase I may be partially reconciled in the Thr-200 → His (T200H) mutant of isozyme II, which exhibits kinetic characteristics for CO_2 hydration tending toward those measured for isozyme I (Behravan et al., 1990). Interestingly, the substitution of Thr-200 in CAII with Ile, Ala, Gly, His, Arg and Ser gives rise to increased esterase activity as measured by the hydrolysis of *p*-nitrophenylacetate (PNPA); the 7-fold increase measured for Thr-200 → Arg CAII is greater than that of any other naturally occurring variant of carbonic anhydrase (Behravan et al., 1991).

We report here the kinetic characteristics and the three-dimensional structure of the Thr-200 → Ser (T200S) mutant of CAII. This mutant exhibits CO_2 hydrase activity that is essentially identical with that of the wild-type enzyme; however, it displays a 4-fold increase in esterase activity relative to the wild-type enzyme. An unexpected result of the X-ray crystallographic structure determination is the significant conformational change of His-64 that accompanies the T200S mutation. Given that the imidazole side chain of His-64 is about 5 Å away from the hydroxyl side chain of Thr-200 in wild-type CAII, it appears that the conformation of His-64 is particularly sensitive to changes in the surrounding solvent and/or counterion structure. Furthermore, the implication of mobility for His-64 may be relevant to the understanding of catalysis and inhibition in the CAII active site.

Materials and Methods

Mutagenesis. The cloned CAII gene (Murakami et al., 1987; a generous gift of Dr. W. S. Sly) was placed under T7 regulatory control by inserting it between a T7 late promoter and terminator (Fierke et al., 1991; Nair et al., 1991; Rosenberg et al., 1987). Oligonucleotide-directed "spiked" random mutagenesis (Caruthers et al., 1987) was performed by using a 62-base oligonucleotide encoding amino residues 190–210 synthesized with 0.8% of each of the three incorrect nucleotides at each step to give an overall doping of 2.4% at each position. In vitro mutagenesis was performed according to the method of Stannsens et al. (1989), and the resulting DNA was transformed into WK6 *mutS* cells. The entire CAII gene was sequenced by the dideoxy method of Sanger et al. (1977) and showed only a single mutation in the codon for position 200 (ACC → TCC).

Phenotypic Screening of Mutants. Mutant plasmid DNA was transformed into BL21(DE3) pLysS cells (Studier & Moffatt, 1986). Resulting colonies were plated onto nitrocellulose filters (Young & Davis, 1983; Singh et al., 1989) and grown overnight at 37 °C, and then the filters were transferred onto induction media/agar plates [20 g/L tryptone, 10 g/L yeast extract, 5 g/L NaCl, 0.5 × M9 salts (Maniatis et al., 1982), 1 mM $MgSO_4$, 0.5% glucose, 2 mM IPTG, 0.3 mM $ZnSO_4$, 100 μg/mL ampicillin, and 25 μg/mL chloramphenicol), incubated at 31–34 °C for 4 h, and the cells were lysed by a freeze/thaw procedure. The esterase activity of CAII in each colony was assessed by overlaying a paper filter soaked in 0.02 mg/mL fluorescein diacetate (Guilbault & Kramer, 1964) in 5% methyl cellusolve/95% 25 mM Tris-SO_4, pH 7.4, incubating for 5 min, and then visualizing the fluorescein product under a medium-wave (320-nm) UV light. Functionally altered CAII variants are readily detected by comparison to control colonies containing either WT or no CAII.

Enzyme Induction and Purification. A 15-L culture of BL21(DE3) pLysS cells containing a plasmid encoding T200S CAII was incubated in induction medium to $A_{600} = 1$. CAII was induced by addition of 1 mM IPTG and 0.3 mM $ZnSO_4$ and incubation for 5 h at 34 °C. Cells were pelleted, resuspended in $^1/_{50}$ volume of lysis buffer (50 mM Tris-SO_4, pH 8.0, 50 mM NaCl, 5 mM EDTA, 0.1% Triton X-100, 1 mM DTT, 0.4 μg/mL phenylmethanesulfonyl fluoride and 0.2 mg/mL lysozyme), and incubated at 4 °C for 1.5–2 h followed by addition of DNase I (final concentration = 0.01 mg/mL). Cellular remnants were removed from the extract by centrifugation at 20000*g* for 20 min. Enzyme was purified from crude cellular lysates by using sulfonamide affinity chromatography as previously described (Osborne & Tashian, 1975). The concentration of CAII was determined by measuring the absorbance at 280 nm and using a molar absorptivity of 5.4×10^4 M^{-1} cm^{-1} (Coleman, 1967).

Esterase Assays. The k_{cat}/K_M for CAII-catalyzed PNPA hydrolysis was measured at 25 °C in either 50 mM Tris-SO_4 (pH 7–9) or 50 mM MES (pH 5.5–7), $\mu = 0.1$ with $NaSO_4$, by measuring the change in A_{348}/min ($\epsilon = 5000$ M^{-1} cm^{-1}) as a function of PNPA concentration (0–0.5 mM) (Armstrong et al., 1966). The pK_a and pH-independent k_{cat}/K_M were calculated by using eq 1 and the statistical program SYSTAT (Systat, Inc.).

$$(k_{cat}/K_M)_{obs} = \frac{k_{cat}/K_M}{1 + 10^{pK_a - pH}} \quad (1)$$

Inhibitor Binding. Dansylamide (DNSA) binding constants were determined by measuring an increase in fluorescence (excitation = 280 nm, emission = 470 nm) upon binding of DNSA to CAII (Chen & Kernohan, 1967) at 25 °C in 20 mM Tris-SO_4 buffer, pH 8.0, with concentrations of CAII 5-fold less than the observed K_D. Binding constants and error estimates were determined by using the Kaleidagraph (Synergy Software) curve-fitting program with eq 2. Acetazolamide (ACET) binding can be measured by competition with bound DNSA as a decrease in fluorescence (excitation = 280 nm, emission = 470 nm) indicative of a decrease in the concentration of the E·DNSA complex. The acetazolamide dissociation constant can be calculated from this data by using eq 3; where Fl is the observed fluorescence, EP is the fluorescence

$$Fl = \frac{EP}{\left(1 + \frac{K_{DNSA}}{[DNSA]}\right)} + BF \quad (2)$$

$$Fl = \frac{IF}{1 + \frac{K_{DNSA}}{[DNSA]}\left(1 + \frac{[ACET]}{K_{ACET}}\right)} + BF \quad (3)$$

endpoint, IF is the initial fluorescence, BF is the background fluorescence, and K_{DNSA} and K_{ACET} are the dissociation constants for dansylamide and acetazolamide binding, respectively.

The K_{azide}^{obs} was calculated from the sodium azide inhibition of CAII-catalyzed PNPA hydrolysis at 0.5 mM PNPA, 50

mM MES, pH 7.0, μ = 0.1 with Na_2SO_4, 25 °C, by using eq 4.

$$\text{rate} = \frac{k_{cat}/K_M}{1 + \frac{[\text{azide}]}{K^{obs}_{azide}}} \quad (4)$$

CO_2/HCO_3^- Exchange. The kinetic constants for the CAII-catalyzed exchange between CO_2 and HCO_3^- at equilibrium, k_{cat}^{exch}, $K_{eff}^{HCO_3^-}$, and $k_{cat}^{exch}/K_{eff}^{HCO_3^-}$, were determined by the ^{13}C NMR line-broadening technique (Koenig et al., 1974) as previously described by Simonsson et al. (1979) with the following modifications: buffer conditions used were 0.1 M MES, pH 7.35, μ = 0.2 with Na_2SO_4, 25 °C, in 10% D_2O and initial enzyme concentrations ranged from 23 to 37 μM. ^{13}C spectra were obtained on a GN 300 wide-bore spectrometer.

CO_2 Hydration. Initial rates of CO_2 hydration were measured in a KinTek stopped-flow apparatus (designed by Ken Johnson, The Pennsylvania State University) at 25 °C by the changing pH-indicator method (Khalifah, 1971). The reaction was monitored at 578 nm in 50 mM TAPS buffer (pH 8.5) with 25 μM *m*-cresol purple, 0.1 mM EDTA, μ = 0.1 M with Na_2SO_4. The CO_2 concentration (3–27 mM) and the TAPS concentration (5–100 mM) were varied. Copper inhibition of CO_2 hydrase activity was measured at 400 nm in 5 mM HEPES, pH 7.5, 48 μM *p*-nitrophenol, μ = 0.1, 25 °C, with the addition of up to 10 μM copper.

Crystallography. Recombinant wild-type and mutant CAIIs were crystallized by the sitting-drop method. A typical crystallization procedure involved the addition of a 20-μL drop containing 0.3 mM enzyme, 50 mM Tris-HCl (pH 8.0 at room temperature), 150 mM NaCl, and 3 mM NaN_3 to a 20-μL drop containing 50 mM Tris-HCl (pH 8.0 at room temperature), 150 mM NaCl, and 3 mM NaN_3 with 1.75–2.5 M $(NH_4)_2SO_4$ in the crystallization well. Both solutions were saturated with methylmercury acetate in order to facilitate the growth of diffraction-quality parallelepipedons. Additionally, the addition of 0.1 mM octyl β-glucoside (McPherson et al., 1986) to the enzyme buffer was required for the crystallization of the mutant enzyme. Crystals of typical dimensions 0.2 mm × 0.2 mm × 0.8 mm appeared within 2 weeks at 4 °C. Wild-type and mutant CAIIs crystallized in space group $P2_1$ and exhibited typical unit cell parameters of a = 42.7 Å, b = 41.7 Å, c = 73.0 Å, and β = 104.6°.

Crystals were mounted and sealed in 0.5-mm glass capillaries with a small portion of mother liquor. A Siemens X-100A multiwire area detector, mounted on a three-axis camera and equipped with Charles Supper double X-ray focusing mirrors, was used for data acquisition. Copper Kα radiation was produced by a Rigaku RU-200 rotating anode X-ray generator operating at 45 kV and 65 mA. All data were collected at room temperature by the oscillation method; the crystal-to-detector distance was set at 14 cm and the detector swing angle was fixed at 25° in two data collection runs and at 20° in four additional runs. Data frames of 0.1° oscillation about ω were collected, with exposure times of 60 s/frame, for total angular rotation ranges about ω of at least 70° per run. Five data sets for wild-type CAII and six data sets for T200S CAII were collected, and diffraction intensities were measured to limiting resolutions of 2.1 Å for each structure. Raw data frames were analyzed by using the BUDDHA package (Durbin et al., 1986) and replicate and symmetry-related structure factors were merged by using the software PROTEIN (Steigemann, 1974); final merging R factors of 0.092 and 0.081 were calculated for wild-type CAII and the T200S mutant, respectively. Relevant data reduction statistics for the mutant enzyme are recorded in Table I.

Table I: Data Collection and Refinement Statistics

	wild-type CAII	T200S CAII
no. of crystals	3	2
no. of measured reflections	20760	33370
no. of unique reflections	10200	10725
maximum resolution (Å)	2.1	2.1
$R_m(F)^a$	0.092	0.081
no. of water molecules in final cycle of refinement	102	119
no. of reflections used in refinement (6.5–2.1 Å)	9346	9932
R factor[b]	0.183	0.166
RMS deviation from ideal bond lengths (Å)	0.026	0.020
RMS deviation from ideal bond angles (deg)	1.9	1.9
RMS deviation from ideal planarity (Å)	0.012	0.008
RMS deviation from ideal chirality (Å^3)	0.140	0.079

[a] R_{merge} for data sets for replicate reflections, $R = \sum||F_{hi}| - \langle|F_h|\rangle|/\sum\langle|F_h|\rangle$; $|F_{hi}|$ = scaled structure factor for reflection h in data set i, $\langle|F_h|\rangle$ = average structure factor for reflection h calculated from replicate data. [b] Crystallographic R factor, $R = \sum||F_o| - |F_c||/\sum|F_o|$; $|F_o|$ and $|F_c|$ are the observed and calculated structure factors, respectively.

The structure of recombinant wild-type CAII was refined at 2.1-Å resolution by using the refined structure of the blood enzyme as a starting point (Eriksson et al., 1986, 1988a; atomic coordinates were generously provided by Dr. T. Alwyn Jones). The final crystallographic R factor for the wild-type enzyme structure was 0.183; details of this work will be reported elsewhere (R. S. Alexander, S. K. Nair, and D. W. Christianson, unpublished experiments).

For the structure determination of T200S CAII, structure factors obtained from corrected intensity data were used to generate difference electron density maps by using Fourier coefficients $(2|F_o| - |F_c|)$ and $(|F_o| - |F_c|)$ with phases calculated from the final refined model of recombinant wild-type CAII. The atoms of residue 200 as well as active-site solvent molecules were deleted from the atomic model prior to the structure factor calculation. Fast Fourier transform routines (Ten Eyck, 1973, 1977) were employed in all electron density map and structure factor calculations. The coordinates of the mutant protein model, including those of the Ser-200 side chain, were adjusted by inspection of difference electron density maps. It was at this stage that the major conformational change of His-64 was noticed, and this observation was confirmed by inspection of maps for which His-64 was omitted from the structure factor calculation.

Model building was performed with the graphics software FRODO (Jones, 1985) installed on an Evans and Sutherland PS390 interfaced to a VAXstation 3500. Atomic coordinates were then refined against the observed data by the reciprocal space least-squares method using the stereochemically restrained least-squares algorithm of Hendrickson and Konnert [1981; also, see Hendrickson (1985)]. Active-site water molecules were not included in the inital stages of refinement. Residue conformations throughout the protein were examined during the course of refinement by using maps calculated with the Fourier coefficients outlined above and phases derived from the in-progress atomic model. Only minimal adjustments to residue conformations were necessary, and active-site water molecules were added when the crystallographic R factor dropped below 0.200. Refinement converged smoothly to a final crystallographic R factor of 0.166; the final model had excellent stereochemistry with rms deviations from ideal bond lengths and angles of 0.02 Å and 1.9°, respectively. Pertinent refinement statistics are recorded in Table I.

Table II: Esterase Activity and Inhibitor Binding

		wild type	T200S
PNPA hydrolysis[a]	k_{cat}/K_M (M^{-1} s^{-1})	2500 ± 200	9700 ± 250
	pK_a	6.74 ± 0.05	6.86 ± 0.05
sulfonamide binding[b]	K_{DNSA} (nM)	850 ± 10	360 ± 10
	K_{ACET} (nM)	8.2 ± 0.3	4.2 ± 0.3
azide inhibition[c]	K_{azide}^{obs} (mM)	0.48 ± 0.13	0.12 ± 0.01
		(0.17)[d]	(0.05)[d]

[a] pK_a and pH-independent k_{cat}/K_M were calculated by using eq 1 at 25 °C, μ = 0.1 with Na_2SO_4. [b] Measured in 20 mM Tris-SO_4 buffer, pH 8.0, 25 °C. [c] Measured from inhibition of PNPA esterase activity in 50 mM MES buffer, pH 7.0, μ = 0.1 with Na_2SO_4, 25 °C. [d] The pH-independent K_{azide} calculated from $K_{azide} = K_{azide}^{obs}/(1 + 10^{pH-pK_a})$.

A difference electron density map calculated with Fourier coefficients ($|F_o| - |F_c|$) and phases derived from the coordinates of the final model revealed that the highest peaks in the vicinity of the active site were just under 3.5σ. The rms error in atomic positions was estimated to be ca. 0.25 Å on the basis of relationships derived by Luzzati (1952). The coordinates of T200S CAII, as well as those of the wild-type enzyme, have been deposited in the Brookhaven Protein Data Bank (reference codes 5CA2 and 4CA2, respectively; Bernstein et al., 1977).

Materials. Fluorescein diacetate and PNPA were obtained from Sigma Chemical Co. Acetazolamide, *p*-nitrophenol, and dansylamide were obtained from Aldrich Chemical Co. Tris base and MES were obtained from Research Organics. Dansylamide and PNPA were purified before use by recrystallization from ethanol and diethyl ether, respectively. All other chemicals were reagent grade.

Results and Discussion

In a screen of a library of CAII variants, substitutions at position 200, including T200S, uniquely gave rise to a phenotype with increased esterase activity (J. F. Krebs and C. A. Fierke, unpublished experiments; Behravan et al., 1990, 1991). The pH-independent rate constant, k_{cat}/K_M, for PNPA hydrolysis catalyzed by T200S CAII (Table II) is 4-fold (0.8 kcal/mol) larger than wild-type, confirming that the esterase activity is enhanced by this mutation. The observed rate of PNPA hydrolysis catalyzed by T200S is linearly dependent on the concentration of PNPA up to 0.5 mM and the pH dependence can be described as a simple titration curve, which is proposed to reflect the ionization of the catalytically important zinc–water ligand (Lindskog, 1966). The increase in k_{cat}/K_M for PNPA hydrolysis could be due either to enhanced binding of the substrate or to an increased catalytic rate constant for ester hydrolysis. The dissociation constants for sulfonamide inhibitors and the inhibition constant for sodium azide (Table II) are decreased 2–5-fold for the T200S mutant compared to wild type. Substitutions of other amino acids at position 200 including Asn, Arg, His, Gly, Ala, Val, and Ile have similar effects on esterase activity and anion binding (Behravan et al., 1990, 1991; J. F. Krebs and C. A. Fierke, unpublished experiments), suggesting that the positioning of the threonine side chain interferes with these activities.

The T200S mutation has minor effects on the kinetics of CAII-catalyzed CO_2 hydration, as summarized in Table III. The steady-state kinetic parameters are virtually identical with those measured for wild type with only a slight decrease in the isotope effect on k_{cat}. The largest effect of the mutation is observed in the kinetic parameters for CO_2/HCO_3^- exchange, k_{cat}^{exch} and $K_{eff}^{HCO_3^-}$, which is best interpreted in the framework of the enzymatic mechanism for wild-type CAII (Silverman & Lindskog, 1988). There is considerable evidence that hydration of CO_2 by CAII consists of two steps; CO_2/HCO_3^- interconversion involving the metal center (eq 5) followed by a proton transfer step to re-form the zinc–hydroxyl enzyme involving first a "proton-shuttle" group and then a buffer-dependent reaction (eq 6) (Silverman & Tu, 1975; Jonsson et al., 1976). Values for the individual rate constants

Table III: CO_2 Hydrase Activity

		wild type	T200S
CO_2 hydration[a]	$k_{cat}/K_M \times 10^{-7}$ (M^{-1} s^{-1})	8.9 ± 0.7	8.6 ± 0.9
	$(k_{cat}/K_M)^H/(k_{cat}/K_M)^D$	1.2 ± 0.2	1.4 ± 0.4
	$k_{cat} \times 10^{-5}$ (s^{-1})	9.3 ± 0.5	8.4 ± 0.5
	$(k_{cat})^H/(k_{cat})^D$	4.3 ± 0.3	3.0 ± 0.4
	$K_M^{CO_2}$ (mM)	11 ± 1	10 ± 2
CO_2/HCO_3^- exchange[b]	$k_{cat}^{exch}/K_{eff}^{HCO_3^-} \times 10^{-6}$ (M^{-1} s^{-1})	4.6 ± 0.7	4.2 ± 0.7
	$k_{cat}^{exch} \times 10^{-5}$ (s^{-1})	6.7 ± 1.7	2.6 ± 0.4
	$K_{eff}^{HCO_3^-}$ (mM)	147 ± 61	62 ± 20

[a] Measured by stopped-flow indicator method (Khalifah, 1971) in 50 mM TAPS buffer, pH 8.5, 25 μM *m*-cresol purple, 0.1 mM EDTA, μ = 0.1 with Na_2SO_4, 25 °C. [b] Measured by ^{13}C NMR line-broadening technique (Simonsson et al., 1979) in 0.1 M MES buffer, pH 7.35, μ = 0.2 with Na_2SO_4, 25 °C, 10% D_2O.

$$E\text{-}OH^- + CO_2 \underset{k_{-1}}{\overset{k_1}{\rightleftharpoons}} E\text{-}HCO_3 \underset{k_{-2}}{\overset{k_2}{\rightleftharpoons}} E\text{-}OH_2 + HCO_3^- \quad (5)$$

$$E\text{-}OH_2 \underset{k_{-3}}{\overset{k_3}{\rightleftharpoons}} +H\text{-}E\text{-}OH^- \underset{k_{-4}[BH]}{\overset{k_4[B]}{\rightleftharpoons}} E\text{-}OH^- \quad (6)$$

in eqs 5 and 6 have been estimated for wild-type enzyme from computer simulations of the kinetic data, and the data in Table III are consistent with this kinetic scheme (Lindskog, 1984; Rowlett, 1984). (The kinetic parameters for CO_2 hydration in Table III are *not* pH-independent constants, but since the mutation does not affect the activity-controlling pK_a, these values allow comparison of mutant to wild type.) For this mechanism at high buffer concentrations, $k_{cat} = k_2k_3/(k_2 + k_3) \approx k_3$ and $k_{cat}/K_M = k_1k_2/(k_{-1} + k_2) \approx k_1$ (since $k_2 > k_3$ and $k_2 > k_{-1}$ for wild type). These kinetic parameters for the T200S mutation are identical with those for the wild type, suggesting that the mutation has no effect on either CO_2 binding/hydration or the intramolecular proton transfer. There is no kinetic evidence for involvement of the methyl group of Thr-200 in CO_2 binding as proposed by Merz (1991) and Liang and Lipscomb (1990) in molecular dynamics studies.

The kinetic parameters for CO_2/HCO_3^- exchange include only the rate constants in eq 5: $k_{cat}^{exch} = k_{-1}k_2/(k_{-1} + k_2) \approx k_{-1}$, $k_{cat}^{ex}/K_{eff}^{HCO_3^-} = k_{-1}k_{-2}/(k_2 + k_{-1}) \approx k_{-1}\,k_{-2}/k_2$, and $K_{eff}^{HCO_3^-} = k_2/k_{-2}$. The decrease in $K_{eff}^{HCO_3^-}$ for the mutant can be readily interpreted as increased binding of HCO_3^- (0.5 kcal/mol) due to either an increase in the HCO_3^- association rate constant, k_{-2}, or a decrease in the HCO_3^- dissociation rate constant, k_2. The latter is more likely since it would account for both an equivalent decrease in k_{-1} (k_{cat}^{exch}) and the observed decreased solvent isotope effect in k_{cat}. (The observed isotope effect is dependent on the intrinsic isotope effect and the ratio of k_3/k_2.) Taken together, these results indicate that increased stabilization of the E·HCO_3^- complex, consistent with the increased binding of other anions, is the major effect of the T200S mutation. Increased stabilization of this complex is also observed in the T200H mutant (Behravan et al., 1990), suggesting that the methyl group of the β-branched threonine may sterically interfere with the bound HCO_3^- molecule in the wild-type enzyme.

The kinetic data for CO_2 hydration clearly indicate that the T200S mutation has no effect on the intramolecular proton transfer, k_3. This is intriguing in light of the large conformational change observed in the crystal for the side chain of

His-64, the amino acid that functions as the proton acceptor. To further investigate the functional properties of His-64 in the T200S mutant, the dependence of CO_2 hydration on the concentration of TAPS buffer was measured showing little or no effect of the mutation: $k_{cat}/K_M^{buffer} = (1.7 \pm 0.1) \times 10^8$ M^{-1} s^{-1} (WT) and $(2.4 \pm 0.1) \times 10^8$ M^{-1} s^{-1} (T200S). This essentially measures k_4 in eq 6 and shows that the rate constant for proton transfer between His-64 and solvent is also virtually unaffected by the conformational change. Finally, copper inhibition of CO_2 hydration, proposed to be due to cupric ions binding to His-64 (Tu et al., 1981, 1989), was measured for both enzymes: 50% inhibition occurs at 1.7 μM (T200S) or 1.8 μM (WT) cupric sulfate at pH 7.5. Therefore, despite the mobility of His-64, the overall kinetic behavior of T200S CAII is equivalent to that of the wild-type enzyme.

The three-dimensional structure of T200S CAII is quite similar to that of wild-type CAII, with the occasional exception of some surface residues. This is not an unusual result, since surface residues often appear disordered in electron density maps and hence experience conformational variation in crystallographic refinement. Least-squares superposition of the wild-type and T200S C_α coordinates [with the software INSIGHT (Biosym, Inc.)] yields an rms difference of 0.14 Å between the two structures. Given the rms coordinate error of ca. 0.25 Å calculated from relationships derived by Luzzati (1952), the rms differences measured between the wild-type and mutant enzymes suggest that the two structures are essentially identical. The protein zinc coordination polyhedra of each structure are likewise similar, and zinc–imidazole distances (Table IV) are generally within experimental error of the average value (Zn^{2+}–N, 2.0 Å) determined in a survey of the Cambridge Structural Database (Vedani & Huhta, 1990). In both wild-type and T200S CAII, a mercury ion binds to Cys-206. It must be emphasized that this is not the inhibitory binding location of Hg^{2+}, which is reported to be at His-64 (Eriksson, 1986, 1988b). Moreover, the binding of mercury to Cys-206 does not result in significant structural differences between recombinant wild-type Hg^{2+}-carbonic anhydrase II and Hg^{2+}-free human carbonic anhydrase II (R. S. Alexander, S. K. Nair, and D. W. Christianson, unpublished experiments), so no attempts were made to dialyze the mercury ion out of the crystal prior to X-ray data acquisition.

As seen in Table I, the structure of T200S CAII possesses excellent stereochemistry. A difference electron density map calculated with Fourier coefficients $(2|F_o| - |F_c|)$ and phases derived from the final model of the mutant enzyme is found in Figure 1. Not unexpectedly, there are only minor differences in the conformation of residue 200 in wild-type and T200S CAIIs: for Thr-200 of the wild-type enzyme, $\phi = -134°$, $\psi = 155°$, and $\chi_1 = 62°$; for Ser-200 of T200S CAII, $\phi = -141°$, $\psi = 153°$, and $\chi_1 = 69°$. Torsion angles χ_1 are near optimal values tabulated by Ponder and Richards (1987). These differences, in addition to minor reorganization of the Ser-197–Cys-206 loop, result in the placement of the γ-hydroxyl side chain of Ser-200 in the mutant at a position 0.9 Å away from that of the γ-hydroxyl group of Thr-200 in the wild-type enzyme. Each hydroxyl side chain makes a 3.9-Å van der Waals contact with a solvent molecule. Additionally, the γ-methyl group of Thr-200 makes van der Waals contacts with the backbone carbonyl oxygen of Thr-199, the phenolic hydroxyl of Tyr-7, and three solvent molecules. Although Ser-200 of the mutant lacks a γ-methyl group, the positions of Thr-199 and Tyr-7 do not change in T200S CAII.

Overall, the active-site solvent structure is generally identical among native blood (Eriksson et al., 1986, 1988a), wild-type, and T200S CAIIs—refined solvent positions generally correlate to within 0.5–1 Å among the three structures, and this includes the solvent molecules that make van der Waals contacts with residue 200. No concerted changes in solvent structure are evident that would indicate a response to the T200S mutation, e.g., no solvent molecules appear to move into the "void" created by the deletion of the Thr-200 methyl group. Interestingly, significant electron density is not observed in T200S CAII for the so-called "deep" water molecule, which is found at the mouth of the hydrophobic pocket of native human and wild-type CAIIs (Eriksson et al., 1988a; R. S. Alexander, S. K. Nair, and D. W. Christianson, unpublished experiments); this water hydrogen bonds to zinc-bound hydroxide and is presumably displaced by substrate (Lindskog, 1986). Additionally, significant electron density corresponding to one of the two solvent molecules bridging zinc-bound hydroxide and His-64 in the native blood enzyme [water 318; see Eriksson et al., (1986, 1988a)] is not apparent in wild-type and T200S CAIIs. However, this observation does not imply a catalytic compromise since the wild-type enzyme exhibits normal proton transfer kinetics. Finally, we note that the pK_a of zinc-bound solvent is not affected by differences in interpreted solvent structure among native blood, wild-type, and T200S CAIIs (Table II).

Table IV: Zinc–Ligand Distances in Wild-Type and T200S CAIIs

ligand	distance from zinc (Å)	
	WT CAII	T200S CAII
His-94	2.3	2.2
His-96	2.1	2.2
His-119	2.2	2.1
solvent	2.4	2.8

Although water molecules are built into all "solvent" peaks in the electron density maps, it is possible that at least some of these peaks may correspond to disordered or low-occupancy counterions such as chloride or azide. Hence, the term "solvent" may be interpreted broadly to include potential counterions. In particular, the identity of the nonprotein zinc ligand, which is hydroxide ion in the active enzyme, is ambiguous under the conditions required for enzyme crystallization. The azide inhibition constant of PNPA esterase activity was measured under conditions similar to those used for crystallization (50 mM Tris-Cl, pH 8.0, 150 mM sodium chloride, 2 M sodium sulfate, 25 °C): $K_{azide}^{obs} = 2.9 \pm 0.8$ mM (WT) and 1.5 ± 0.2 mM (T200S). Since these inhibition constants approximate binding constants (Coleman, 1967), the percentage of enzyme under crystallization conditions with azide as the nonprotein ligand can be estimated as 50% (WT) or 67% (T200S). The majority of the remaining molecules should be in the zinc–hydroxyl form since the pH is well above the pK_a for both enzymes and the binding constant for chloride is large (≥0.5 M) at this pH (Behravan et al., 1990). Hence, the nonprotein zinc ligand observed in the crystal structures is actually an equilibrium mixture of different anions, and these equilibrium populations are reapportioned slightly in response to the T200S mutation. The refined position of the nonprotein zinc ligand places it 2.4 and 2.8 Å away from zinc in wild-type and T200S CAIIs, respectively. The peak corresponding to the nonprotein zinc ligand is somewhat asymmetric and egg-shaped in each structure (this peak in T200S CAII is visible in Figure 1); the asymmetry of this peak may be due to a mixed population of zinc-bound counterions.

As mentioned previously, a significant nonlocal difference is observed in T200S CAII: the side chain of His-64 rotates away from the active site by 105° about χ_1 (Figure 1). This conformational change apparently requires the displacement

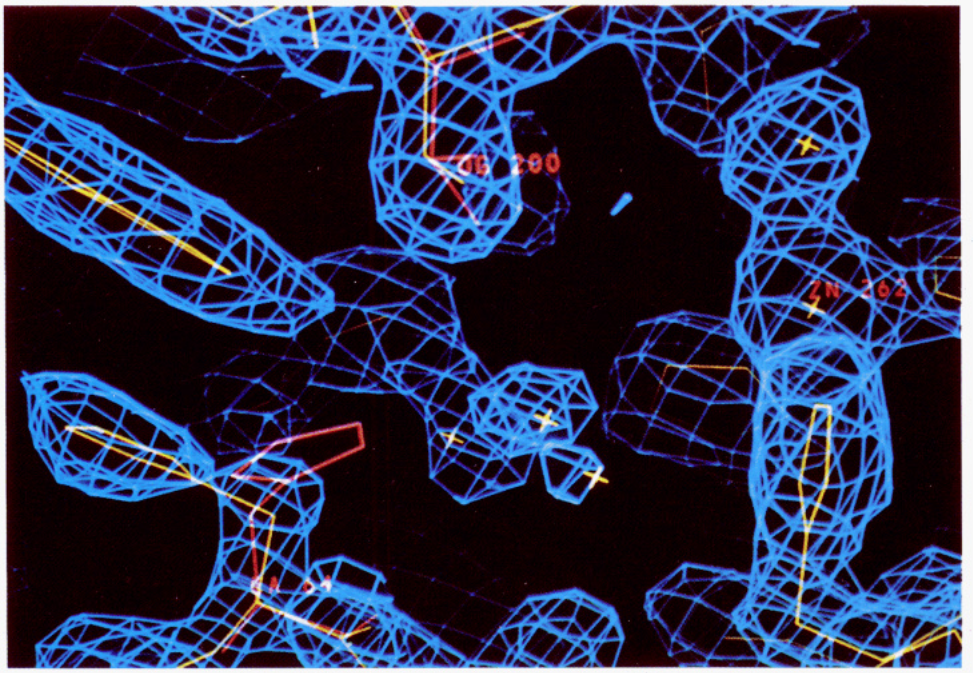

FIGURE 1: Difference electron density map of T200S CAII calculated with Fourier coefficients ($2|F_o| - |F_c|$) and phases derived from the final model. The refined atomic coordinates are superimposed on the map (yellow model); for comparison, the refined coordinates of wild-type CAII are superimposed at positions 64 and 200 (red model). Note the dramatic conformational change of His-64 accompanying the T200S mutation.

of a water molecule observed in wild-type and native blood CAIIs (Eriksson et al., 1986, 1988a). It is not clear why the side chain of His-64, which is at least 5 Å away from the side chain of Thr-200 in the wild-type enzyme, undergoes such a dramatic conformational change in response to the T200S mutation. Although the two conformations of the His-64 side chain are characterized by torsion angles χ_1 and χ_2 (wild-type CAII values are 54° and −92°, respectively; T200S CAII values are −51° and −68°, respectively) that are close to optimal values summarized by Ponder and Richards (1987), no additional structural factors are apparent that would favor the alternate conformation of His-64. For instance, His-64 does not appear to make any hydrogen bonds in its new position as judged from distance and stereochemical criteria (Baker & Hubbard, 1984; Ippolito et al., 1990). Moreover, the alternate position for His-64 places its imidazole side chain in a more hydrophobic region largely defined by Trp-5, Gly-6, Tyr-7, and Phe-231. The conformational change of His-64 is not a general response to point mutations in the enzyme active site, since no change is observed in crystal structures of other CAII mutants at residues Val-143 (R. S. Alexander, S. K. Nair, and D. W. Christianson, unpublished experiments) or Val-121 (Nair et al., 1991), where mutant enzymes were crystallized under conditions identical with those employed for T200S CAII. It is also unlikely that the slight reapportionment of the composition of the nonprotein zinc ligand in T200S would cause this conformation change.

In addition to the interpretation of His-64 mobility in T200S CAII, it is possible to interpret mobility for this residue in crystallographic studies of wild-type and native blood CAIIs due to an ambiguity in solvent assignment. To demonstrate, a difference electron density map of wild-type CAII, calculated with Fourier coefficients ($|F_o| - |F_c|$) and phases derived from the final model less the atoms of His-64 and a neighboring water molecule (O338), reveals that the alternate conformation of His-64 observed in T200S CAII can be superimposed on the electron density corresponding to water O338 modeled in the wild-type enzyme (Figure 2). Therefore, it is a real

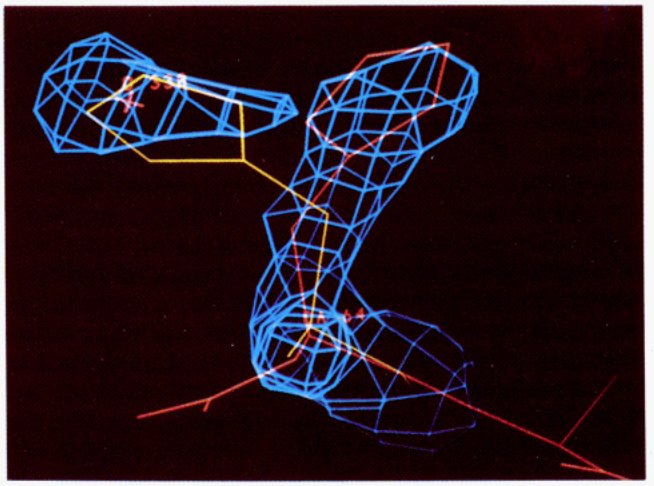

FIGURE 2: Difference electron density map of recombinant wild-type CAII calculated with Fourier coefficients ($|F_o| - |F_c|$) and phases derived from the final model. The atoms of residue His-64 as well as a neighboring water molecule (O338) were omitted from the structure factor calculation, and the map is contoured at 3σ. The refined atomic coordinates of the wild-type enzyme are superimposed on the map (red model), and the alternate conformation of His-64 observed in T200S CAII is also superimposed (yellow model). Note that water O338 of the wild-type enzyme is interpretable as a minor-occupancy, alternate conformation of His-64.

possibility that the nonspherical density interpreted as water O338 in the wild-type enzyme represents a minor-occupancy conformation (ca. 20%) of His-64. Although the conformational change of His-64 as herein reported is observed to be sterically required for the binding of certain sulfonamide inhibitors (Baldwin et al., 1989), results at pH 5.7 and pH 6.5 indicate that conformational changes of His-64 similarly occur even when not sterically required by ligand binding (S. K. Nair and D. W. Christianson, unpublished experiments). Since in wild-type CAII the predominant conformer of His-64 is directed toward the active site, we designate this the "in" conformer; in T200S CAII, His-64 is directed away from the

active site, so we designate this the "out" conformer.

Although we have demonstrated that His-64 is capable of mobility, it is difficult to establish the causal relationship between the T200S mutation and the conformation of His-64. There is no direct hydrogen-bond interaction between Thr-200 and His-64, but these residues flank opposite sides of a solvent-filled cleft in the CAII active site. A plausible hypothesis might be that the conformation of His-64 and its surrounding solvent structure (including both water and counterions) are interdependent. If this is the case, different conformations observed for His-64 in different crystallographic studies may arise from the slight 0.5–1-Å differences in active-site solvent structure observed between wild-type and T200S CAIIs. Furthermore, effects between His-64 and solvent may involve dynamically behaved solvent molecules that are indistinguishable from background density in electron density maps.

Despite the mobility of His-64 and accompanying changes in its surrounding solvent structure, kinetic measurements indicate that efficient proton transfer is sustained in wild-type and T200S CAIIs. In addition to mobility about χ_1, rotational flips about χ_2 for aromatic side chains occur at rates exceeding 10^6 s^{-1} (Gall et al., 1982), so mobility about both χ_1 and χ_2 for His-64 could be sufficiently rapid to remain undetected during steady-state turnover. Kinetic measurements on His-64 → Ala CAII further imply that mobility for His-64 and its surrounding solvent structure is catalytically acceptable in wild-type CAII (Tu et al., 1989). Since the CO_2 hydrase activity of this variant is virtually restored in imidazole buffer (imidazole in solution would correspond to an infinitely mobile histidine side chain), it is likely that efficient catalysis tolerates the relatively minor conformational mobility of His-64 observed or implied in structural studies of wild-type and mutant CAIIs.

The conformational mobility inferred for His-64 of CAII is reminiscent of similar inferences regarding the conformation of His-119 in ribonuclease. In X-ray crystallographic studies at 2-Å resolution, two conformers (designated as "high" and "low" occupancy sites) were initially reported for this residue; these two conformers differed by a rotation of 142° about χ_1 in the enzyme structure refined at 1.45-Å resolution (Wyckoff et al., 1970; Borkakoti et al, 1982, 1983). In contrast, the results of independent crystallographic investigations of anion-free ribonuclease at 1.5-Å resolution (Campbell & Petsko, 1987) and at 1.26-Å resolution (Wlodawer et al., 1988) suggest that only one position for His-119 can be interpreted in electron density maps. Wlodawer et al. (1988) note that an alternate conformation of His-119 could be traced through a nearby water molecule but argue against this alternative on the basis of the observed solvent structure of phosphate-free ribonuclease. However, the results of theoretical calculations (Brunger et al., 1985) and recent crystallographic studies (Kuriyan et al., 1991; S. K. Burley and G. A. Petsko, unpublished experiments) support a two-conformer interpretation for His-119 in ribonuclease. Here, as in CAII, the crystallographic interpretation of histidine side chains may be ambiguous as the distinction between multiple conformations and hydrogen-bonded solvent molecules is made.

Summary and Conclusions

The T200S mutant of CAII exhibits CO_2 hydrase activity that is comparable to that of the wild-type enzyme and esterase activity that is 4-fold greater than that of wild-type enzyme. The three-dimensional structure of T200S reveals a major conformational change for His-64 (about 5 Å from the mutated side chain), which places the imidazole ring of this group in a hydrophobic region of the protein structure defined in part by Trp-5, Gly-6, Tyr-7, and Phe-231; in catalysis, such a conformation might facilitate proton transfer away from His-64 to buffer. Proton transfer is maintained in the T200S CAII mutant, despite the conformational change of His-64, and proton transfer is similarly maintained in the His-64 → Ala CAII by the addition of infinitely mobile imidazole buffer (Tu et al., 1989), suggesting that this reaction is not dependent on the specific ground-state conformers of His-64 visualized in the X-ray structure. Hence, it is conceivable that conformational mobility of the imidazole side chain, accompanied by subtle and compensatory changes in surrounding solvent structure, may accompany the role of His-64 as a catalytic proton shuttle.

Acknowledgments

We thank Drs. James Springer, Brian McKeever, and Anzhi Wei for many helpful discussions.

References

Armstrong, J. M., Myers, D. V., Verpoorte, J. A., & Edsall, J. T. (1966) *J. Biol. Chem. 241*, 5137–5149.

Baldwin, J. J., Ponticello, G. S., Anderson, P. S., Christy, M. E., Murcko, M. A., Randall, W. C., Schwam, H., Sugrue, M. F., Springer, J. P., Gautheron, P., Grove, J., Mallorga, P., Viader, M.-P., McKeever, B. M., & Navia, M. A. (1989) *J. Med. Chem. 32*, 2510–2513.

Baker, E. N., & Hubbard, R. E. (1984) *Prog. Biophys. Mol. Biol. 44*, 97-179.

Behravan, G., Jonsson, B.-H., & Lindskog, S. (1990) *Eur. J. Biochem. 190*, 351–357.

Behravan, G., Jonsson, B.-H., & Lindskog, S. (1991) *Eur. J. Biochem. 195*, 393–396.

Bernstein, F. C., Koetzle, T. F., Williams, G. J. B., Meyer, E. F., Brice, M. D., Rodgers, J. R., Kennard, O., Shimanouchi, T., & Tasumi, M. (1977) *J. Mol. Biol. 112*, 535–542.

Borkakoti, N., Moss, D. S., & Palmer, R. A. (1982) *Acta. Crystallogr. B38*, 2210–2217.

Borkakoti, N., Palmer, R. A., Haneef, I., & Moss, D. S. (1983) *J. Mol. Biol. 169*, 743–755.

Brunger, A.T., Brooks, C. L., & Karplus, M. (1985) *Proc. Natl. Acad. Sci.* U.S.A. 82, 8458–8462.

Campbell, R. L., & Petsko, G. A. (1987) *Biochemistry 26*, 8579–8584.

Caruthers, M. H., Barone, A. D., Beaucage, S. L., Dodds, D. R., Fisher, E. F., McBride, L. J., Matteucci, M., Stabinsky, Z., & Tang, J.-Y. (1987) *Methods Enzymol. 154*, 287–326.

Chen, R. F., & Kernohan, J. C. (1967) *J. Biol. Chem. 242*, 5813–5823.

Christianson, D. W. (1991) *Adv. Protein Chem. 42*, 281–355.

Coleman, J. E. (1967) *J. Biol. Chem. 242*, 5212–5219.

Coleman, J. E. (1986) in *Zinc Enzymes* (Bertini, I., Luchinat, C., Maret, W., & Zeppezauer, M., Eds.) pp 49–58, Birkhauser, Boston.

Durbin, R. M., Burns, R., Moulai, J., Metcalf, P., Freymann, D., Blum, M., Anderson, J. E., Harrison, S. C., & Wiley, D. C. (1986) *Science 232*, 1127–1132.

Eigen, M., & Hammes, G. G. (1963) *Adv. Enzymol. Relat. Subj. Biochem. 25*, 1–38.

Eriksson, A. E., Jones, T. A., & Liljas, A. (1986) in *Zinc Enzymes* (Bertini, I., Luchinat, C., Maret, W., & Zeppezauer, M., Eds.) pp 317–328, Birkhauser, Boston.

Eriksson, A. E., Jones, T. A., & Liljas, A. (1988a) *Proteins: Struct., Funct., Genet. 4*, 274–282.

Eriksson, A. E., Kylsten, P. M., Jones, T. A., & Liljas A. (1988b) *Proteins: Struct., Funct., Genet. 4*, 283–293.

Fierke, C. A., Krebs, J. F., & Venters, R. A. (1991) in *International Workshop on Carbonic Anhydrase II: From Biochemisty and Genetics to Physiology and Clinical Medicine* (Botrē, F., Gros, G., & Storey, B. T., Eds.) pp 22–36, VCH, Weinheim, Germany.

Gall, C. M., Cross, T. A., DiVerdi, J. A., & Opella, S. J. (1982) *Proc. Natl. Acad. Sci. U.S.A. 79*, 101–105.

Guilbault, G. G., & Kramer, D. N. (1964) *Anal. Chem. 36*, 409–412.

Hendrickson, W. A. (1985) *Methods Enzymol. 115*, 252–270.

Hendrickson, W. A., & Konnert, J. (1981) in *Biomolecular Structure, Conformation, Function, and Evolution* (Srinivasan, R., Ed.) Vol. 1, pp 43–57, Pergamon, Oxford, England.

Hewett-Emmett, D., & Tashian, R. E. (1991) in *The carbonic anhydrases: Cellular physiology and molecular genetics* (Dodgson, S. J., Gros, G., Carter, N. D., & Tashian, R. E., Eds.) Plenum, New York (in press).

Ippolito, J. A., Alexander, R. S., & Christianson, D. W. (1990) *J. Mol. Biol. 215*, 457–471.

Jones, T. A. (1985) *Methods Enzymol. 115*, 157–171.

Jonsson, B.-H., Steiner, H., & Lindskog, S. (1976) *FEBS Lett. 64*, 310–314.

Khalifah, R. G. (1971) *J. Biol. Chem. 246*, 2561–2573.

Koenig, S. H., Brown, R. D., London, R. E., Needham, T. E., & Matwiyoff, N. A. (1974) *Pure Appl. Chem. 40*, 103–113.

Kuriyan, J., Osapay, K., Burley, S. K., Brunger, A. T., Hendrickson, W. A., & Karplus, M. (1991) *Proteins: Struct., Funct., Genet. 10*, 340–358.

Liang, J.-Y., & Lipscomb, W. N. (1988) *Biochemistry 27*, 8676–8682.

Liang, J.-Y., & Lipscomb, W. N. (1990) *Proc. Natl. Acad. Sci. U.S.A. 87*, 3675–3679.

Liljas, A., Kannan, K. K., Bergsten, P.-C., Waara, I., Fridborg, K., Strandberg, B., Carlbom, U., Jarup, L., Lovgren, S., & Petef, M. (1972) *Nature, New Biol. 235*, 131–137.

Lindskog, S. (1966) *Biochemistry 5*, 2641–2646.

Lindskog, S. (1984) *J. Mol. Catal. 23*, 357–368.

Lindskog, S. (1986) in *Zinc Enzymes* (Bertini, I., Luchinat, C., Maret, W., & Zeppezauer, M., Eds.) pp 307–316, Birkhauser, Boston.

Luzzati, P. V. (1952) *Acta. Crystallogr. 5*, 802–810.

Maniatis, T., Fritsch, E. F., & Sambrook, J. (1982) *Molecular Cloning*, Cold Spring Harbor Press, Cold Spring Harbor, NY.

McPherson, A., Koszelak, S., Axelrod, H., Day, J., Williams, R., Robinson, L., McGrath, M., & Cascio, D. (1986) *J. Biol. Chem. 261*, 1969–1975.

Merz, K. M., Jr. (1990) *J. Mol. Biol. 214*, 799–802.

Merz, K. M., Jr. (1991) *J. Am. Chem. Soc. 113*, 406–411.

Murakami, H., Marelich, G. P., Grubb, J. H., Kyle, J. W., & Sly, W. S. (1987) *Genomics 1*, 159–166.

Nair, S. K., Calderone, T. L., Christianson, D. W., & Fierke, C. A. (1991) *J. Biol. Chem.* (in press).

Osborne, W. R. A., & Tashian, R. E. (1975) *Anal. Biochem. 64*, 297–303.

Ponder, J. W., & Richards, F. M. (1987) *J. Mol. Biol. 193*, 775–791.

Rosenberg, A. H., Lade, B. N., Chui, D.-S., Lin, S.-W., Dunn, J. J., & Studier, F. W. (1987) *Gene 56*, 125–135.

Rowlett, R. S. (1984) *J. Protein Chem. 3*, 369–393.

Sanger, F., Nicklen, S., & Coulson, A. R. (1977) *Proc. Natl. Acad. Sci. U.S.A. 74*, 5463–5467.

Silverman, D. N., & Tu, C. K. (1975) *J. Am. Chem. Soc. 97*, 2263–2269.

Silverman, D. N., & Lindskog, S. (1988) *Acc. Chem. Res. 21*, 30–36.

Simonsson, I., Jonsson, B.-H., & Lindskog, S. (1979) *Eur. J. Biochem. 93*, 409–417.

Singh, H., Clerc, R. G., & LeBowitz, J. H. (1989) *BioTechniques 7*, 252–261.

Stanssens, P., Opsomer, C., McKeown, Y. M., Kramer, W., Zabeau, M., & Fritz, H.-J. (1989) *Nucleic Acids Res. 17*, 4441–4454.

Steigemann, W. (1974) Ph.D. Thesis, Technische Universitat, Munchen, Germany.

Steiner, H., Jonsson, B.-H., & Lindskog, S. (1975) *Eur. J. Biochem. 59*, 253–259.

Studier, F. W., & Moffatt, B. A. (1986) *J. Mol. Biol. 189*, 113–130.

Ten Eyck, L. F. (1973) *Acta Crystallogr. A29*, 183–191.

Ten Eyck, L. F. (1977) *Acta Crystallogr. A33*, 486–492.

Tu, C. K., Wynns, G. C., & Silverman, D. N. (1981) *J. Biol. Chem. 256*, 9466–9470.

Tu, C. K., Silverman, D. N., Forsman, C., Jonsson, B.-H., & Lindskog, S. (1989) *Biochemistry 28*, 7913–7918.

Vedani, A., & Huhta, D. W. (1990) *J. Am. Chem. Soc. 112*, 4759–4767.

Wlodawer, A., Svensson, L. A., Sjolin, L., & Gilliland, G. L. (1988) *Biochemistry 27*, 2705–2717.

Wyckoff, H. W., Tsernoglou, D., Hanson, A. W., Knox, J. R., Lee, B., & Richards, F. M. (1970) *J. Biol. Chem. 245*, 305–328.

Young, R. A., & Davis, R. W. (1983) *Proc. Natl. Acad. Sci. U.S.A. 80*, 1194–1198.